An Overview of Neural Network Based Modeling in Alloy Design and Thermomechanical Processing of Austenitic Stainless Steels

Article *in* Materials and Manufacturing Processes · January 2009

DOI: 10.1080/10426910802612361

CITATIONS
12

READS
232

4 authors:

Sumantra Mandal
Indian Institute of Technology Kharagpur
130 PUBLICATIONS **4,266** CITATIONS
SEE PROFILE

Sivaprasad Palla
SWERIM
86 PUBLICATIONS **1,996** CITATIONS
SEE PROFILE

P. Barat
162 PUBLICATIONS **1,427** CITATIONS
SEE PROFILE

Baldev Raj
Indira Gandhi Centre for Atomic Research
919 PUBLICATIONS **18,386** CITATIONS
SEE PROFILE

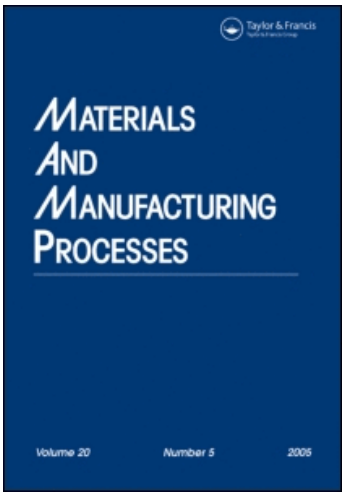

Materials and Manufacturing Processes
Publication details, including instructions for authors and subscription information:
http://www.informaworld.com/smpp/title~content=t713597284

An Overview of Neural Network Based Modeling in Alloy Design and Thermomechanical Processing of Austenitic Stainless Steels

Sumantra Mandal [a]; P. V. Sivaprasad [a]; P. Barat [b]; Baldev Raj [a]
[a] Metallurgy and Materials Group, Indira Gandhi Centre for Atomic Research, Kalpakkam, India [b] Variable Energy Cyclotron Centre, Kolkata, India

Online Publication Date: 01 February 2009

To cite this Article Mandal, Sumantra, Sivaprasad, P. V., Barat, P. and Raj, Baldev(2009)'An Overview of Neural Network Based Modeling in Alloy Design and Thermomechanical Processing of Austenitic Stainless Steels',Materials and Manufacturing Processes,24:2,219 — 224
To link to this Article: DOI: 10.1080/10426910802612361
URL: http://dx.doi.org/10.1080/10426910802612361

Materials and Manufacturing Processes, 24: 219–224, 2009

ISSN: 1042-6914 print/1532-2475 online
DOI: 10.1080/10426910802612361

Taylor & Francis
Taylor & Francis Group

An Overview of Neural Network Based Modeling in Alloy Design and Thermomechanical Processing of Austenitic Stainless Steels

Sumantra Mandal[1], P. V. Sivaprasad[1], P. Barat[2], and Baldev Raj[1]

[1]*Metallurgy and Materials Group, Indira Gandhi Centre for Atomic Research, Kalpakkam, India*
[2]*Variable Energy Cyclotron Centre, Kolkata, India*

This overview reports some of the research works carried out by us in recent past on the application of artificial neural network (ANN) based modeling in alloy design and thermomechanical processing of austenitic stainless steels. Different ANN models were created in order to simulate various correlations and phenomena in austenitic stainless steels. These include: prediction of mechanical properties of alloy D9 from its alloy content, modeling constitutive flow behavior of austenitic stainless steels, and prediction of torsional flow behavior of type 304L stainless steel. Attempt has been made to explain the simulated results by relevant fundamental metallurgical phenomena.

Keywords Alloy composition; Alloy design; Artificial neural network (ANN); Austenitic stainless steel; Constitutive flow behavior; Deformation behavior; Flow stress; Mechanical property; Modeling simulation; Process variables; Recrystallization; Thermomechanical processing; Torsion.

1. Introduction

It has long been known that the mechanical properties of austenitic stainless steels at room temperature and at elevated temperature are related to their alloy composition. The addition of alloying elements to this steel alters the strength of the austenite as 1) the element can dissolve interstitially or substitutionally to form a single phase solid solution so that the austenite is strengthened and 2) the elements can combine with carbon to form fine precipitates so that austenite is strengthened by precipitation strengthening. However, to date, limited progress has been made in predicting the mechanical properties of materials from their alloy content from physical metallurgy point of view. This is due to the complexity of the relationship between the mechanical properties of the material and the alloy content. Further, non-availability of the relative contributions of the two mechanisms as well as synergistic influence of the alloying elements and the two strengthening mechanisms makes the prediction difficult.

Thermomechanical processing like rolling, forging, and extrusion are extensively used in the first step of converting a cast ingot into a wrought product. Understanding the constitutive flow behavior, linking process variables such as strain, strain rate, and temperature to the flow stress of the deforming materials is necessary in order to determine the load required to carry out these operations. Warm and hot deformation behavior of materials is always associated with various interconnecting metallurgical phenomena like work hardening, flow instabilities, dynamic recovery (DRV), dynamic recrystallization (DRX), and thereby complex in nature. In the past, various internal state variables phenomenological models [1, 2] or empirical/semi-empirical equations [3, 4] have been developed to predict the constitutive flow behavior of materials during hot working. Although these approaches attempt to represent the nonlinear relations between flow stress, strain rate, strain, and temperature, these are usually restricted to some limited processing domain where a specific deformation mechanism operates and breaks down across deformation mechanism domains. Therefore, separate equations and/or various equation parameters are needed to represent the complete hot deformation behavior.

In the light of the above discussion, artificial neural network (ANN) provides an efficient alternative. Recently, ANN has been successfully applied to model different metallurgical phenomena in a wide range of metals and alloys [5–11]. This overview reports some of the research works carried out by us in the recent past on the application of ANN-based modeling in alloy design and thermomechanical processing of austenitic stainless steels. Different models were created in order to simulate various correlations and phenomena in austenitic stainless steels. These include: prediction of mechanical properties of alloy D9 from its alloy content, modeling constitutive flow behavior of austenitic stainless steels, and prediction of torsional flow behavior of type 304L stainless steel. Since designed models are "statistical" models, i.e., they are not based on any physical theories, simulated results from the models have been explained by relevant fundamental metallurgical phenomena.

2. Methodology

A Gaussian process model was employed to predict the tensile properties of alloy D9 from its alloy content. This modeling technique has found a variety of applications in the field of materials science [12, 13]. We have adopted a Bayesian approach in the model, which allows: (1) automatic control of the complexity of the nonlinear model; (2) calculation of error bars describing the reliability of the model prediction; (3) automatic determination of the relevance of the various input variables. A three-layer feed-forward network, on the other hand, has been employed

Received February 26, 2008; Accepted September 10, 2008
Address correspondence to Sumantra Mandal, Metallurgy and Materials Group, Indira Gandhi Centre for Atomic Research, Kalpakkam, TN 603102, India; Fax: +91 44 27480075; E-mail: sumantra@igcar.gov.in

to develop the ANN models related to thermomechanical processing discussed in this article. The feed-forward networks were trained by back-propagation type algorithm. A logistic sigmoid function, expressed as, $f(x) = \frac{1}{1+\exp(-x)}$, was employed as the activation function.

3. Results and discussion

3.1. Prediction of Mechanical Properties of Alloy D9

The aim of this study is to predict the tensile properties of alloy D9 (20% cold worked) at room temperature and at 923 K from its alloy content namely C, Ti, Ni, Cr, and Mn. To this end, alloys of different compositions with varying C levels in the range 0.026–0.13 and Ti/C ratios in the range 3–8 were prepared in Balzer's VSG30 vacuum induction melting (VIM) and casting unit. Button head type specimens of 26 mm gauge length and 4 mm gauge diameter were employed for tensile testing. Tensile tests were carried out on 20% cold worked condition in a universal testing machine, at a strain rate of $3.14 \times 10^{-4}\,s^{-1}$ at room temperature as well as at 923 K. The details of experiments, testing, and data evaluation could be found elsewhere [14]. The input parameters of the model are the alloy composition while the yield strength (YS), ultimate tensile strength (UTS), percentage uniform elongation (UE%), percentage total elongation (TE%), and percentage reduction in area (RA%) were obtained as the output.

The Gaussian Process model was run using data from 70 samples each at room temperature and at 923 K of different alloy content for the prediction of various tensile properties of alloy D9. Normally to assess the predictive capability of such a model, half the data is used for training and the other half for testing. However, our data set is too small to train the model on just half of the data and hence, we have used a one-by-one analysis technique, which still has the virtue that the model has no prior knowledge of the outcome of the test results. In this procedure, 69 data sets are used for training and the outcome of the 70th value of the concerned mechanical property is predicted. This procedure is then repeated for each of the other 70 data sets. The results of the prediction of 70 similar models are plotted as the true values on the X-axis and the predicted data on the Y-axis. Figure 1 shows a typical plot of true against predicted data for UTS for the specimens tested at room temperature. On this figure, the difference between the true value and the predicted value is denoted as ΔZ. This is also the distance of the ordinate of the predicted value from the straight line (AB) having gradient equal to one. In certain circumstances, the plot of predicted vs. measured data exhibits a strong level of correlation, but the gradient is not equal to one. The straight line CD is the least squared fitted line of the predicted results having a gradient m. ΔY is the distance of the ordinate of the predicted points from this line. The Gaussian process model also estimates the uncertainty (standard deviation σ) of the prediction of each datum. Consequently, the following metrics have been used, and the uncertainty (R, r and $\langle(\Delta Z/\sigma)\rangle$) has been estimated based on the following mathematical formulae:

$$R = \frac{1}{N}\left\{\sum(\Delta Z)^2\right\}^{\frac{1}{2}} \tag{1}$$

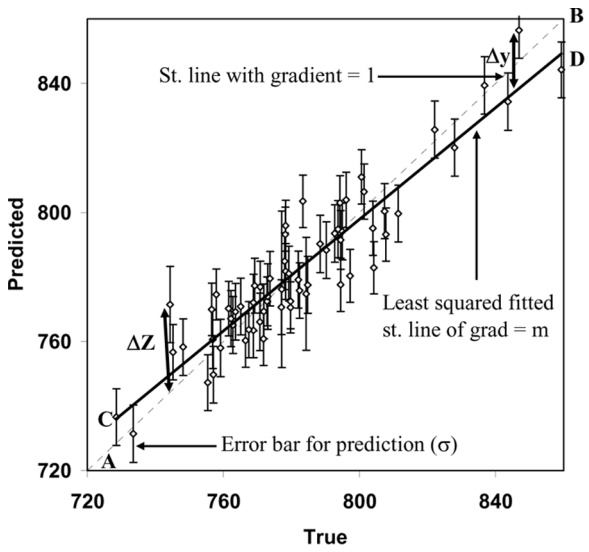

Figure 1.—True against predicted values of UTS at room temperature on which the schematic depiction of how the metrics are estimated is shown.

$$r = \frac{1}{N}\left\{\sum(\Delta Y)^2\right\}^{\frac{1}{2}} \tag{2}$$

$$\langle(\Delta Z/\sigma)\rangle = \frac{1}{N}\left\{\sum(\Delta Z/\sigma)^2\right\}^{\frac{1}{2}}, \tag{3}$$

where N is the number of data points. In principle, for the ideal case, the gradient m should be one and the other coefficients R and r should be zero. The coefficient R measures the root mean square (rms) error in the prediction and r measures the rms deviation of the predicted points from the least squared fitted straight line. The rms $\langle(\Delta Z/\sigma)\rangle$ is useful because large differences between the model and the observed value are more serious when the model has inferred a high level of certainty in the prediction, while large differences between the model and the observed value would be expected if a large uncertainty was associated with the prediction of that point. Thus $\langle(\Delta Z/\sigma)\rangle$ also signifies the average number of standard deviations from which the predicted value differs from the target value.

Figure 2 shows True vs. Predicted values of UTS at 923 K. The estimated values of the metrics R, r, and $\langle(\Delta Z/\sigma)\rangle$ for different predictions are given in Table 1. The metrics in this table obviously demonstrate that the models for the prediction of various mechanical properties have generalized well, and therefore have captured the underlying relationships in the training data. In Table 1, the values of the metrics at the bottom are for absolutely correlated and random vectors. These values give the idea of the two extreme possible values of the metrics. From this table, it is quite apparent that the predictions of YS, UTS, UE% (at 923 K), and UTS measured at room temperature are very good. In general, the predictions are better for the mechanical properties of D9 materials measured at 923 K. Uncertainties in the predictions of mechanical properties are mainly due to the noise present in the data set.

Table 2 gives the relevance of the different alloying elements in the prediction of different mechanical

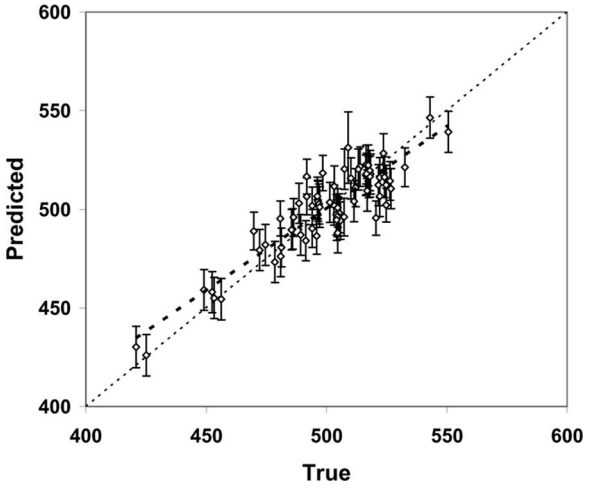

FIGURE 2.—True against predicted values of UTS at 923 K.

properties. The relevance factors mentioned in the Table 2 are in the form of numbers ranging from 1 (highest relevance) to 5 (least relevance) according to its importance. From Table 2, it could be seen that C shows high relevance for the prediction of almost all the mechanical properties compared to any other alloying elements present in the matrix. C dissolves interstitially in the austenitic phase and interstitial strengthening is superior to substitutional strengthening in austenite. Hence, the observed high relevance of C from the models matches with the well established knowledge of Metallurgy. The observed relevance of C for the prediction of the different mechanical properties at 923 K is more than that observed at room temperature (RT). This is attributed to the fact that at 923 K the formation of fine TiC precipitates is expected which contributes to better elevated temperature properties. It can also be noticed that higher relevance of Ti at 923 K is also due to the same effect. Therefore, it is demonstrated that the model is robust and the findings are well in conformity with the fundamental metallurgical understanding. In contrast, Cr has shown higher relevance for strength at RT when compared to those at 923 K. This is due to the fact that solid solution strengthening is responsible for RT strength and strength due to precipitation

TABLE 1.—The values of the metrics for the predictions of the mechanical properties.

Mechanical properties	R	r	$\langle \Delta Z/\sigma \rangle$	M
YS (RT)	0.0149	0.0119	0.1416	0.607
YS (923 K)	0.0090	0.0084	0.124	0.8592
UTS (RT)	0.0099	0.0092	0.143	0.8454
UTS (923 K)	0.0092	0.0085	0.123	0.8304
UE% (RT)	0.0212	0.0152	0.143	0.4749
UE% (923 K)	0.0112	0.0103	0.142	0.8468
TE% (RT)	0.0184	0.0139	0.1368	0.5158
TE% (923 K)	0.0211	0.0153	0.140	0.4542
RA% (RT)	0.0183	0.0144	0.138	0.5831
RA% (923 K)	0.0170	0.0108	0.141	0.3595
Correlated vectors	1.46×10^{-5}	1.46×10^{-5}	0.007	1
Random vectors	0.0634	0.0307	0.3115	−0.0152

TABLE 2.—Relevance of the different elements for the predictions of the mechanical properties.

Mechanical properties	Relevance of elements at RT					Relevance of elements at 923 K				
	C	Ti	Ni	Cr	Mn	C	Ti	Ni	Cr	Mn
YS	2	4	5	1	3	1	2	3	5	4
UTS	1	5	2	3	4	1	3	2	5	4
UE%	2	3	1	4	5	1	5	3	4	2
TE%	1	2	4	3	5	1	4	5	3	2
RA%	1	2	3	5	4	1	5	4	2	3

is not possible owing to higher affinity of C for the formation of TiC. Ni showed higher relevance for UTS at room temperature and at 923 K compared to YS. This is attributed to the change in the strain-hardening behavior with Ni or increase in toughness with Ni. According to the established metallurgical knowledge Ni generally increases the ductility and toughness. Mn showed higher relevance for ductility (UE%, TE%) at 923 K compared to the observed relevance at room temperature from the models. This observation is absolutely in conformity with the existing knowledge of metallurgy, which states that Mn improves ductility.

It is very difficult to analyze the effect of the variation of the weight percentage of only one alloying element on the mechanical properties experimentally. This is because to study this effect experimentally, one has to prepare samples in which only the concentration of that particular element is varied systematically whereas the concentration of all other elements shall remain same. This is very difficult to realize in practice. However, with our model we could simulate this effect by systematically varying the alloying composition and predicting the properties. Towards this end, we trained the model with the existing data and predicted the mechanical properties when the weight percentage of four of the alloying elements was kept constant but the weight percentage of the fifth element was varied systematically. From these exercises, we could also find the optimum choice of the composition to get best values of YS and UTS for D9 alloy at room temperature and at 923 K. Typical results of this analysis are given in Table 3. This is particularly useful while designing new alloys with specified tensile properties.

3.2. Constitutive Flow Behavior of Austenitic Stainless Steels

A feed forward ANN model has been developed to simulate the correlations between alloy compositions, process variables, and flow stress of austenitic stainless steels under hot compression. The input parameters of the

TABLE 3.—Optimum choice of the alloy composition to get higher values of YS and UTS obtained from the model at 923 K and room temperature (RT).

C	Ti	Ni	Cr	Mn	YS	UTS	Condition
0.05	0.32	14.96	15.23	1.39	501.8		923K
0.05	0.31	14.94	15.22	1.37		521.4	923K
0.08	0.32	14.69	15.74	1.56	743.0		RT
0.13	0.20	15.67	15.57	1.20		805.0	RT

ANN are alloy compositions (C, Ni, Cr, Mo, Ti, and N) and process variables (strain, strain rate, and temperature). The output is flow stress. A comprehensive database (2128 datasets) has been employed to establish this model. A very good correlation between the experimental and the predicted data was obtained. The correlation coefficient for training and test data are 0.995 and 0.993, respectively. On the other hand, average absolute relative error for training and test dataset are found to be 4.65% and 4.82%, respectively. Since test data were not used for training, it essentially verified the ability of any ANN model to associate and generalize a true physical response. The details of the ANN model is given elsewhere [15].

The developed model was employed to simulate the influence of alloying elements on flow behavior of austenitic stainless steel. Influence of Ni (wt%) on the flow behavior of type 304 stainless steel at various temperature is shown in Fig. 3. As can be seen, flow stress decreases with addition of Ni. It is known that increasing the Ni content increases the stacking-fault energy (SFE) [16] of materials. This increase in SFE, in turn, facilitates the cross slip of extended dislocations. As a result, the number of dissociated dislocations in the matrix decreases which eventually leads to lower rate of work hardening. The influence of N on flow behavior of type 316L(N) austenitic stainless steel is depicted in Fig. 4. It can be observed that addition of N, particularly in lower hot working temperature range, increases flow stress. This is attributed to the solid solution strengthening effect of N. The movements of dislocations are readily impeded in presence of N which eventually increases the flow stress. At higher temperature, however, marked influence of N is not observed. This could be ascribed to the higher thermal energy available in these temperature ranges that facilitates to overcome the barrier offered by nitrogen. The effect of Ti on flow behavior in alloy D9 is shown in Fig. 5. At low temperature, increase in Ti causes reduction in flow stress while no significant effect of Ti is observed at high temperature. Addition of Ti causes TiC precipitates in the matrix during straining. The TiC precipitates enhance the rate of nucleation that eventually

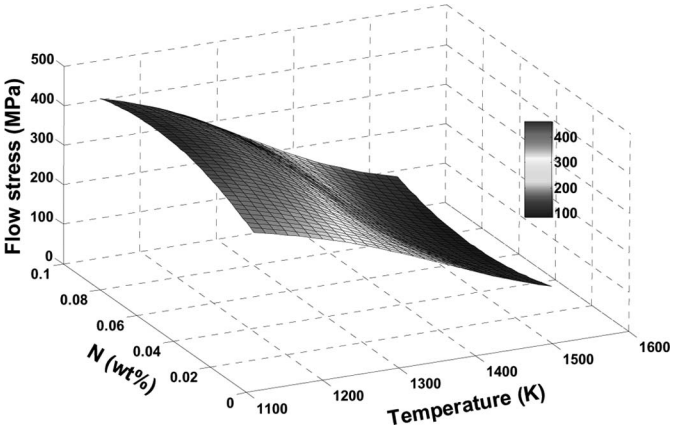

FIGURE 4.—Influence of N (wt%) on flow stress in type 316L(N) stainless steel at various temperatures (strain: 0.3 and strain rate: $10\,s^{-1}$).

favors DRX [17]. At high temperature, on the other hand, available thermal activation energy is sufficient enough to supersede the effect of Ti, and therefore no significant effect on flow stress is observed.

3.3. Torsional Flow Behavior of Type 304L Stainless Steel

The flow behavior of a material also depends on the state of stress, and therefore the deformation behavior of materials during torsion differs significantly from that in compression. For example, it is well known that axial stresses develop during torsion of a bar with end constraints [18]. The state-of-stress in torsion would therefore be biaxial, and yield occurs at lower stresses than in compression. At lower temperatures and higher strain rates, the material exhibits flow instabilities which are more accentuated in torsion than in compression. In addition, the flow stresses in torsion are lower because of the absence of friction and a contribution from the reduced polar moment of inertia of the cross-section due to the undeformed central

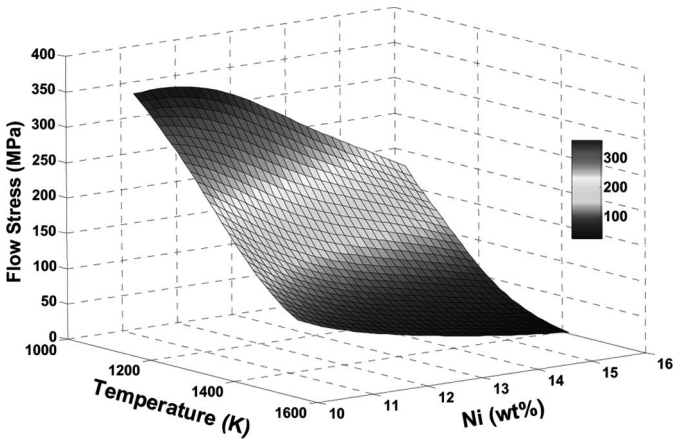

FIGURE 3.—Influence of Ni (wt%) on flow stress in type 304 stainless steel at various temperatures (strain: 0.5 and strain rate: $10\,s^{-1}$).

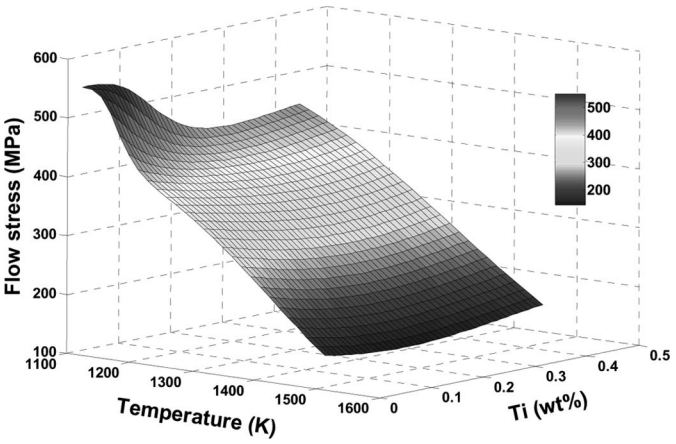

FIGURE 5.—Influence of Ti (wt%) on flow stress in alloy D9 at various temperatures (strain: 0.5 and strain rate: $100\,s^{-1}$).

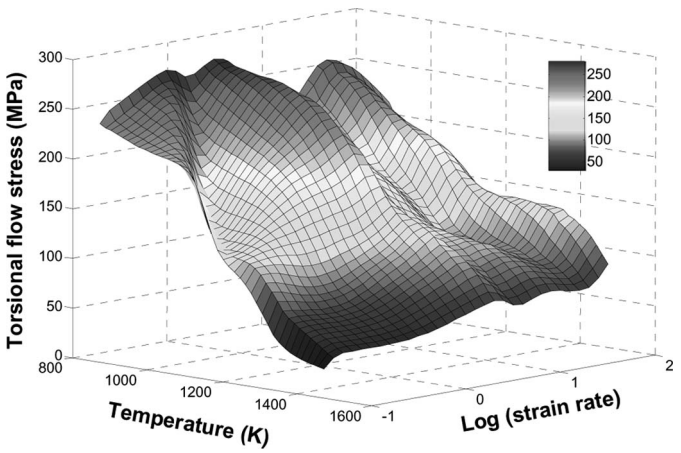

FIGURE 6.—Combined influence of temperature and strain rate on torsional flow behavior of 304L stainless steel at a strain of 0.2.

region [18, 19]. Therefore, an attempt has been made to predict the deformation behavior of type 304L stainless steel under warm and hot torsion using ANN. The inputs of the model are strain, log strain rate, and temperature while torsional flow stress is obtained as output. A three layer feed-forward network has been trained with resilient propagation algorithm. Best performances were obtained after incorporating 16 neurons in the hidden layer. The correlation coefficient for training and test data are 0.9963 and 0.9948, respectively. Further, average absolute relative error for training and test dataset are found to be 3.79% and 4.16%, respectively. The details of the ANN model can be found in [20].

Synergistic influence of temperature and strain rate on torsional flow behavior of 304L stainless steel has been simulated employing the developed ANN model. The results at 0.2 strain level is shown in Fig. 6. Almost similar trends were obtained at 0.3 and 0.5 strain levels [17]. This emphasises the fact that strain hardening is not significant during hot deformation. Figure 6 reveals negative strain rate sensitivity in lower temperature regime (873–1073 K). This could be attributed to the flow localization that causes instability in the flow behavior of materials. The flow localization in torsion arises due to the fact that the state-of-stress in torsion is essentially shear, which accentuates shear localization. In fact, torsion test is considered to be ideal for assessing the susceptibility of a material to undergo flow localization [21]. The instability in the flow behavior at 1273 K, particularly in the strain rate regime of 10–100 s^{-1}, probably arises due to ferrite formation. It has already been shown that ferrite formation is favored in torsion as compared to compression [22]. These ferrites are formed due to the deformation heating at this higher strain rate level. At 1473 K, the trend is quite regular, which signifies that flow behavior in this temperature regime is mainly governed by work hardening and dynamic softening. As strain rate increases, the extent of dynamic softening reduces, which eventually increases the flow stress.

4. CONCLUSIONS

Application of neural network based modeling in alloy design and thermomechanical processing of austenitic stainless steels were discussed. The following are the conclusions:

1) The database obtained from the tensile testing of the laboratory heats was employed to develop a Gaussian process model to correlate alloy composition with tensile properties of alloy D9 at room temperature and at 923 K. The model is particularly useful while designing new alloys with specified tensile properties.
2) An ANN model was developed to predict the constitutive flow behavior of austenitic stainless steels during hot deformation. The input parameters were alloy composition and process variables whereas flow stress is the output. The model can be used as a guideline to develop new alloys with specific flow properties.
3) An ANN model was developed to evaluate and predict the deformation behavior under warm and hot torsion of AISI type 304L stainless steel as a function of process variables. The model provides very useful information to choose desired thermomechanical processing domain of this material.

REFERENCES

1. Mecking, H.; Kocks, U.F. Kinetics of flow and strain-hardening. Acta Metallurgica **1981**, *29* (11), 1865–1875.
2. Estrin, Y.; Mecking, H. A unified phenomenological description of work hardening and creep based on one-parameter models. Acta Metallurgica **1984**, *32* (1), 57–70.
3. Rao, K.P.; Hawbolt, E.B. Development of constitutive relationships using compression testing of a medium carbon steel. Transaction ASME Journal of Engineering Materials Technology **1992**, *114*, 116–123.
4. Davenport, S.B.; Silk, N.J.; Sparks, C.N.; Sellars, C.M. Development of constitutive equations for modelling of hot rolling. Materials Science and Technology **2000**, *16*, 539–546.
5. Pal, D.; Datta, A.; Sahay, S.S. An efficient model for batch annealing using a neural network. Materials and Manufacturing Processes **2006**, *21* (5), 567–572.
6. Mousavi Anijdan, S.H.; Madaah-Hosseini, H.R.; Bahrami, A. Flow stress optimization for 304 stainless steel under cold and warm compression by artificial neural network and genetic algorithm. Materials and Design **2007**, *28* (2), 609–615.
7. Sheikh-Ahmad, J.; Twomey, J. ANN constitutive model for high strain-rate deformation of Al 7075-T6. Journal of Materials Processing Technology **2007**, *186* (1–3), 339–345.
8. Orbanic, P.; Fajdiga, M. A neural network approach to describing the fretting fatigue in aluminium-steel couplings. International Journal of Fatigue **2003**, *25* (3), 201–207.
9. Ravi, R.; Prasad, Y.V.R.K.; Sarma, V.V.S. An artificial neural network (ANN) model for predicting instability regimes in copper–aluminum alloys. Materials and Manufacturing Processes **2007**, *22* (7), 846–850.
10. Mandal, S.; Sivaprasad, P.V.; Dube, R.K. Kinetics, mechanism and modelling of microstructural evolution during thermomechanical processing of a 15Cr-15Ni-2.2Mo-Ti modified austenitic stainless steel. Journal of Materials Science **2007**, *42*, 2724–2734.

11. Mehta, R.; Sahay, S.S.; Datta, A; Chodha, A. Neural network models for industrial batch annealing operation. Materials and Manufacturing Processes **2008**, *23* (2), 203–208.
12. Cool, T.; Bhadeshia, H.K.D.H.; Mackay, D.J.C. The yield and ultimate tensile strength of steel welds. Materials Science and Engineering **1997**, *223* (1–2), 186–200.
13. Bhadeshia, H.K.D.H.; Mackay, D.J.C.; Svensson, L.E. The impact toughness of C–Mn steel arc welds – A Bayesian neural network analysis. Materials Science and Technology **1995**, *11* (10), 1046.
14. Sivaprasad, P.V.; Mandal, S.; Venugopal, S; Narayanan, C.; Shanmugam, V.; Raj, B. Artificial neural network modelling of the tensile properties of indigenously developed 15Cr-15Ni-2.2Mo-Ti modified austenitic stainless steel. Trans. Indian Inst. Met. **2006**, *59* (4), 437–445.
15. Mandal, S.; Sivaprasad, P.V.; Venugopal, S.; Murthy, K.P.N. Constitutive flow behaviour of austenitic stainless steels under hot deformation: Artificial neural network modelling to understand, evaluate and predict. Modelling and Simulation in Materials Science and Engineering **2006**, *14* (6), 1053–1070.
16. Dulieu, D.; Nutting, J. ISI Spec. Rep. **1964**, *86*, 140.
17. Mandal, S.; Sivaprasad, P.V.; Venugopal, S.; Murthy K.P.N.; Raj, B. Artificial neural network modeling of composition-process-property correlations in austenitic stainless steels. Materials Science and Engineering A **2008**, *485*, 571–580.
18. Hardwick, D.; Tegart, W.J. McG. J. Inst. Metals **1961**, *90*, 17.
19. Luton, M.J.; Sellers, C.M. Dynamic recrystallization in nickel and nickel–iron alloys during high temperature deformation. Acta Metallurgica **1969**, *17* (8), 1033–1043.
20. Mandal, S.; Sivaprasad, P.V.; Venugopal, S.; Murthy, K.P.N. Artificial neural network modeling to evaluate and predict the deformation behavior of stainless steel type AISI 304L during hot torsion. Applied Soft Computing **2009**, *9*, 237–244.
21. Semiatin, S.L.; Jonas, J.J. *Formability and Workability of Metals*; ASM: Metals Park, OH, 1984; 13 pp.
22. Venugopal, S. Optimization of Workability and Control of Microstructure in Deformation Processing of Austenitic Stainless Steels: Development and Application of Processing Maps for Stainless Steels Type AISI 304 and 316L. Ph.D. thesis, Department of Mechanical Engineering, University of Madras, 1993.